Chapter 2
Adsorption Isotherms in Liquid Phase: Experimental, Modeling, and Interpretations

Jeferson Steffanello Piccin, Tito Roberto Sant'Anna Cadaval Jr., Luiz Antonio Almeida de Pinto, and Guilherme Luiz Dotto

Abstract Adsorption is a fundamental unit operation used for several purposes in the academy and industry. Particularly, adsorption in liquid phase is used to remove recalcitrant compounds from effluents (dyes, heavy metals, phenols, pharmaceuticals, and others), to recover valuable metals from leachates (gold, silver, cobalt, and others), and to purify products during the industrial processing (fuels, juices, liquors, wines, and others). For all these applications, the obtainment, modeling, and interpretation of the equilibrium isotherms are a key and fundamental study. Based on the abovementioned, this chapter presents the particularities of adsorption equilibrium isotherms in liquid phase from scientific and technological viewpoints. From the scientific viewpoint, the importance of adsorption isotherms will be addressed. For example, the equilibrium isotherms provide parameters for decision-making of the researcher in relation to the adsorption capacity of a particular adsorbent, give an idea how the interaction of adsorbent–adsorbate occurs, and provide means to find thermodynamic parameters, among others. From technological viewpoint, the adsorption capacity of the material is a basic parameter for the project. Thus, in this chapter the following points are highlighted: experimental procedures to obtain equilibrium curves, isotherm analysis, models used to correlate the equilibrium data and interpretation of its parameters, regression methods (comparison between linear and nonlinear regression methods), error analysis, adsorption thermodynamics, and the use of these data for equipment design.

J.S. Piccin
Food Engineering Department, Passo Fundo University, UPF, Br. 285, Km 171, 99052-900, Passo Fundo, RS, Brazil
e-mail: jefersonpiccin@gmail.com

T.R.S. Cadaval Jr. • L.A.A. de Pinto
Industrial Technology Laboratory, School of Chemistry and Food, Federal University of Rio Grande, km 08 Itália Avenue, 96203-900, Rio Grande, RS, Brazil
e-mail: titoeq@gmail.com; dqmpinto@furg.br

G.L. Dotto (✉)
Chemical Engineering Department, Federal University of Santa Maria, 1000 Roraima Avenue, 97105-900, Santa Maria, RS, Brazil
e-mail: guilherme_dotto@yahoo.com.br

A. Bonilla-Petriciolet et al. (eds.), *Adsorption Processes for Water Treatment and Purification*, DOI 10.1007/978-3-319-58136-1_2

Keywords Adsorption • Equilibrium • Isotherms • Liquid phase • Modeling

Contents

2.1 Introduction

Adsorption is a unit operation that involves the contact of a solid phase with a fluid phase (liquid or gas) (Ruthven 1984). In this work, only the solid–liquid adsorption is addressed. The solid phase is known as adsorbent and the liquid phase (the solvent, normally water) contains one or more compounds to be adsorbed (the adsorbates). Due to unbalanced forces, the adsorbate is attracted to the adsorbent surface, and consequently, the degrees of freedom and the surface free energy are reduced (Suzuki 1993). The transference of the adsorbate from the liquid phase to the solid phase continues until the equilibrium to be reached between the amount of adsorbate linked in the adsorbent and the amount of adsorbate remaining in the solution. The affinity degree between the adsorbent and adsorbate determines this distribution in liquid and solid phases (Rouquerol et al. 2014).

In general, the adsorption can be classified according to the type of interaction that occurs between the adsorbent and adsorbate. If there is an electron transfer between the adsorbent and adsorbate, then, it is a chemical adsorption or chemisorption. In this case, the adsorption involves electron transfer, and it is of high energy, ranging from 40 to 800 kJ/mol and, consequently, desorption is difficult, and thus the process is irreversible and only a monolayer is observed. In chemisorption, the interactions can occur mainly by ionic or covalent bonds (Crini and Badot 2008). Otherwise, if no electron exchange is observed, a physical adsorption or physisorption occurs. In this case, the adsorption energies are low, ranging from 5 to 40 kJ/mol and, consequently, desorption is possible and the process can be reversible and multilayer adsorption is possible. In physisorption, the interactions

can be electrostatic, hydrogen bonds, van der Waals, or dipole–dipole (Bergmann and Machado 2015). It should be highlighted that this classification between physical and chemical adsorption is a general behavior, but is not a dogma. Each case should be examined separately.

Several advantages have been cited regarding the adsorption operation. For example, in comparison with other unit operations, the adsorption in liquid medium has a low energetic requirement and its implementation and operation are easy. Many materials can be used as adsorbents, which can be regenerated and reused several times. This practice becomes the adsorption in a low-cost operation. Also, adsorption is efficient since it can remove or recover all the adsorbate from the solution, providing a perfect separation. After, the adsorbent and adsorbate could be reused. In some cases, adsorption is also selective (Do 1998). On the other hand, after the adsorption, an additional operation can be necessary to provide a good solid–liquid separation, for example, filtration, sedimentation, or centrifugation. Another drawback is high cost of activated carbon, the adsorbent most commonly used, mainly due its high surface area. In some cases, a secondary problem can occur with the disposal of the generated sludge (Bansal and Goyal 2005).

To develop an adequate adsorption system, the adsorbent choice is the first and fundamental aspect. A good adsorbent should have the following characteristics: low cost; availability; efficiency; high surface area and pore volume; mechanical, chemical, and thermal stability; ease of desorption and reuse; and able to provide a fast kinetics and, mainly, present a high adsorption capacity (Rodrigues 2015). For this proposal, the activated carbon is the adsorbent most utilized (Bansal and Goyal 2005). Other common adsorbents are clays, silica, and zeolites (Rouquerol et al. 2014). However, in the last years, several researches have been focused on the preparation, characterization, and application of nonconventional adsorbents. Some examples are powdered agro-wastes, powdered industrial wastes, chitosan, chitin, fungi, bacteria, and algae (Dotto et al. 2015a). Surely, these studies are relevant, but, to choose an adequate adsorbent, among other information, the following question is fundamental: in which process the adsorbent will be used?

In operational terms, some configurations are possible for an adsorption process, for example, discontinuous batch adsorption, continuous stirred-tank reactor (CSTR), fixed bed adsorption, expanded bed adsorption, fluidized bed adsorption, simulated moving bed adsorption, and others (Rouquerol et al. 2014; Dotto et al. 2015a; Rodrigues 2015). In this chapter, the discontinuous batch adsorption and the fixed bed adsorption will be addressed, since they account for about 90% of the scientific literature.

Figure 2.1 shows a schematic representation of a discontinuous batch adsorption operation. In this case, a certain amount m of a pure adsorbent is put in contact with a solution with an initial volume V_0 and an initial concentration of adsorbate C_0. The solution is stirred at temperature constant until the end of operation (e.g., the equilibrium). During the operation period, the adsorbate is transferred to the adsorbent surface, decreasing its concentration in the solution until C_e and increasing its quantity in the solid phase until q_e (Crini and Badot 2008).

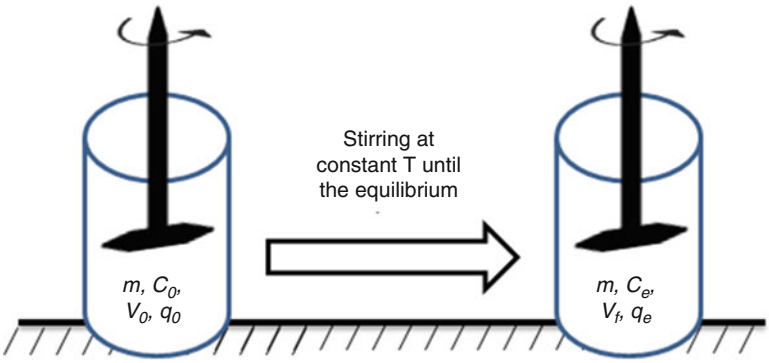

Fig. 2.1 Schematic representation of a discontinuous batch adsorption operation

In discontinuous batch operations, a simple mathematic treatment is normally performed to obtain the amount of adsorbate adsorbed into the adsorbent at equilibrium (q_e). A global mass balance of the adsorbate is given by Eq. (2.1) (Geankoplis 1998):

$$C_0V_0 + q_0m = C_eV_f + q_em \tag{2.1}$$

For a virgin adsorbent, the amount of adsorbate at the beginning is equal to 0, leading to Eq. (2.2):

$$C_0V_0 = C_eV_f + q_em \tag{2.2}$$

or

$$q_e = \frac{C_0V_0 - C_eV_f}{m} \tag{2.3}$$

In the majority of the experimental cases, the aliquot removed for quantification of the adsorbate is negligible regarding the total volume of the solution, leading to $V_0 = V_f = V$. So, the amount of adsorbate adsorbed into the adsorbent at equilibrium is given by Eq. (2.4):

$$q_e = \frac{(C_0 - C_e)V}{m} \tag{2.4}$$

The discontinuous batch adsorption systems are useful and fundamental to verify the quality of an adsorbent and define some operational parameters, such as pH, temperature, amount of adsorbent, and operation time, in laboratory scale. Also it is used for industrial applications for small volumes (Piccin et al. 2009, 2011).

Figure 2.2 shows a schematic representation of a fixed bed adsorption operation. In fixed bed adsorption systems, a solution with initial adsorbate concentration C_0 (normally named influent) is pumped at a flow rate Q, through a column with

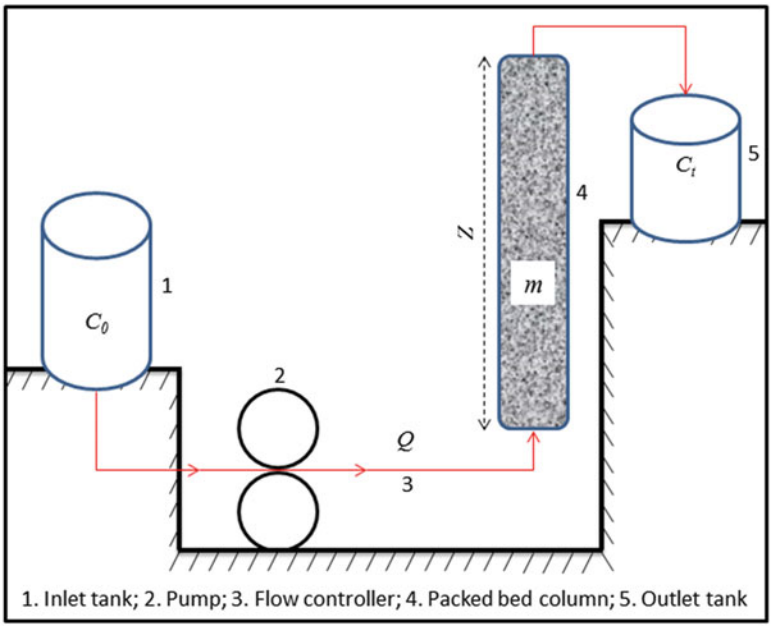

Fig. 2.2 Schematic representation of a fixed adsorption operation

Z height, which is packed with a certain amount m of adsorbent. During the operation, the adsorbate is transferred from the solution to the adsorbate surface. As a consequence, the solution is clarified, achieving an output concentration of C_t. The output solution is normally named effluent. The equilibrium is attained when the bed saturation occurs, i.e., $C_t = C_0$ (Shafeeyan et al. 2014).

In the case of fixed bed operations, the data analysis is performed aiming to obtain the breakthrough time (t_b), exhaustion time (t_e), length of mass transfer zone (Z_m), effluent volume (V_{eff}), maximum capacity of the column (q_{eq}), and removal percentage (R). The breakthrough time (t_b) is considered when the outlet adsorbate concentration attains low levels (in general less than 5%) in relation to the initial concentration, and the exhaustion time (t_e) is considered when the outlet concentration attains 95% of the initial concentration. The Z_m reflects the shortest possible adsorbent bed length needed to obtain the breakthrough time t_b at $t = 0$. The metric length of this zone is calculated by Eq. (2.5) (Worch 2008):

$$Z_m = Z\left(1 - \frac{t_b}{t_e}\right) \tag{2.5}$$

The volume of the effluent, V_{eff}, is given by Eq. (2.6):

$$V_{\text{eff}} = Qt_{\text{total}} \tag{2.6}$$

where t_{total} is the total operation time.

The maximum capacity of the column (q_{eq}) is given by Eq. (2.7):

$$q_{eq} = \frac{QC_0 \int_0^{t_{total}} \left(1 - \frac{C_t}{C_o}\right) dt}{m} \tag{2.7}$$

The integral in Eq. (2.7) is the area above the breakthrough curve from $C_t/C_0 = 0$ to $C_t/C_0 = 1$.

The removal percentage (R) is given by Eq. (2.8) (Dotto et al. 2015b):

$$R = \frac{\int_0^{t_{total}} \left(1 - \frac{C_t}{C_o}\right) dt}{t_{total}} 100 \tag{2.8}$$

The fixed bed systems are useful and fundamental in order to scale up the adsorption operations. The real operational conditions, such as flow rate and bed height, can be simulated, and parameters for scale-up can be obtained. For example, from laboratory fixed bed experiments, it is possible to estimate the column height necessary to obtain a good quality effluent in a determined time. This height can be easily transferred for pilot or industrial scale (Vieira et al. 2014; Dotto et al. 2015b).

To develop an adsorption operation, in discontinuous batch or in fixed bed systems, the first step is the adsorbent choice and the second is the obtainment of the adsorption isotherms. Adsorption isotherms are a relation between the amount of adsorbate adsorbed in the adsorbent (q_e) and the amount of adsorbate remaining in the liquid phase (C_e), when the two phases are in dynamic equilibrium at a determined temperature. In liquid phase adsorption systems, the isotherm curves are important due to the following aspects:

- From the isotherm parameters, it is possible to obtain the maximum adsorption capacity of a determined adsorbent under different experimental conditions. The maximum adsorption capacity is an indicative of the adsorbent quality.
- Also from the isotherm parameters, it is possible to obtain information about the energetic, steric, and affinity viewpoints.
- The isotherm shape can provide information about the interaction mechanism that occurs between the adsorbent and the adsorbate.
- In terms of the adsorption rate modeling, a local equilibrium is generally considered, in order to solve the partial differential equations. This local equilibrium is mathematically described by the adsorption isotherms.
- Thermodynamic adsorption parameters, such as standard Gibbs free energy change (ΔG^0), standard enthalpy change (ΔH^0), and standard entropy change (ΔS^0), can be found from the isotherms. These parameters are fundamental to verify the spontaneity and nature of the adsorption operation.

In the light of this knowledge, the equilibrium isotherms should be examined carefully. Firstly, the equilibrium experiments should be performed with several

experimental points. After, the isotherm curves should be correctly classified. Suitable models should be fitted to the curves, in order to find an adequate representation and consistent parameters. For this, a correct statistic treatment is necessary. Finally, the isotherms can be used to find information about the adsorption operation.

2.2 Experimental Procedures to Obtain Equilibrium Curves

For the construction of adsorption isotherm, it is necessary that a series of equilibrium concentration data of the liquid phase with its respective adsorption capacity is obtained. These data not only should be in temperature equilibrium but also in all other system conditions, such as adsorbent characteristics, agitation, solution volume, and especially pH, in the case of adsorption in liquid phase. Then, in the batch adsorption tests, an adsorbent dosage (m) is mixed with a certain volume (V_0) of a solution at an initial solute concentration (C_0).

In this context, a number of methods have been standardized to obtain the adsorption isotherms and this section will handle some of these methods. The American Society for Testing and Materials (ASTM) reports two methodologies for the determination of adsorption isotherms in liquid phase. The ASTM D-3860 is the standard practice for the determination of adsorptive capacity of activated carbon by aqueous phase isotherm technique. This practice covers the determination of the adsorptive capacity of activated carbon to remove undesirable constituents from water and wastewater. The method suggested by the ASTM, in this case, reports that different adsorbent dosages are placed into contact with a solution containing known solute concentration. Thus, when equilibrium is reached, different values of equilibrium concentrations (C_e) are obtained and the adsorption capacities (q_e) are calculated by Eq. (2.4). According to the method, for the activated carbon, usually after few hours equilibrium is reached. However, the time required for equilibrium to be reached will be treated later.

Already the ASTM D-4706 test method covers the determination of the relative activation level of unused or reactivated carbons by adsorption of iodine from aqueous solution. This test method is based upon a three-point adsorption isotherm, and the standard iodine solution is treated with three different weights of activated carbon under specified conditions, according to the ASTM D-3860. The equilibrium data are processed using the Langmuir model (which will be discussed later) and the iodine number is the maximum adsorption capacity of the monolayer (q_m).

Van Den Hul and Lyklema (1968) and Hang and Brindley (1970) proposed a method for determining the available surface area for adsorption in an aqueous medium based on adsorption isotherm Methylene Blue dye (CAS No. 61-73-4). This method is based on the adsorption of a layer of Methylene Blue on the surface (internal and external) material. Based on the maximum monolayer adsorption

capacity (q_m) obtained by Langmuir model (Eq. (2.18)) that is treated subsequently, it is possible to obtain the number of molecules adsorbed per unit area (the projected area of the Methylene Blue molecule is 1.08×10^{-18} m^2/molecule) and the total area (a_p, in m^2/g) of the adsorbent according to Eq. (2.9):

$$a_p = 1.7388 q_m \tag{2.9}$$

Although the methods of ASTM suggest that the adsorption isotherms are performed by different dosages of adsorbent, more recent works by adsorption, especially those that use nonconventional adsorbents, have chosen to use fixed adsorbent dosages, and different point isotherms are obtained varying the solute initial concentration of the solution. By this method, variations in the adsorption system conditions are less susceptible. In this case, for example, stock solutions containing 300 or 400 mg/L (or more) are diluted in the ratio 1:1 (solution/solvent) obtaining different initial conditions. Both methods (different dosages of adsorbent and different initial concentrations of the solute solution) lead to the same result if the technique is properly developed.

However, we want to draw attention to the considerations regarding the adsorption equilibrium. Several authors have presented data kinetic adsorption capacity justifying that equilibrium is achieved within hours after consecutive measurements performed in relatively short times (few minutes or a few hours) showing similar results. However, we consider that for determining the correct balance, this should be measured in longer periods of time, i.e., from 8 to 12 h, being performed until there are no observed changes in the equilibrium concentration. The evaluation of these changes can be detected by lower coefficients of variation of 5% in the equilibrium concentration in three consecutive measurements, as suggested by some authors.

2.3 Classification of the Equilibrium Isotherms

As described above, the equilibrium isotherms show the amount of adsorbate that can be adsorbed by the adsorbent (q_e) in relation to the equilibrium concentration of the adsorbate in fluid phase (C_e). These are critical parameters in the adsorption system design. Furthermore, the shape of the equilibrium curve helps to explain certain phenomena associated with the interaction between the adsorbate and adsorbent. Therefore, the isotherm shape not only provides information on the affinity between the molecules but also reflects the possible mode of interaction between adsorbate and adsorbent (Wong et al. 2004).

The classification of liquid–solid adsorption isotherms describes a system (Giles et al. 1960) and suggests how their form can be used to diagnose the adsorption mechanism, in order to obtain information regarding the physical nature of the adsorbate and the adsorbent surface and also to measure the specific surface area of the adsorbent. In this classification, the equilibrium curves are identified according

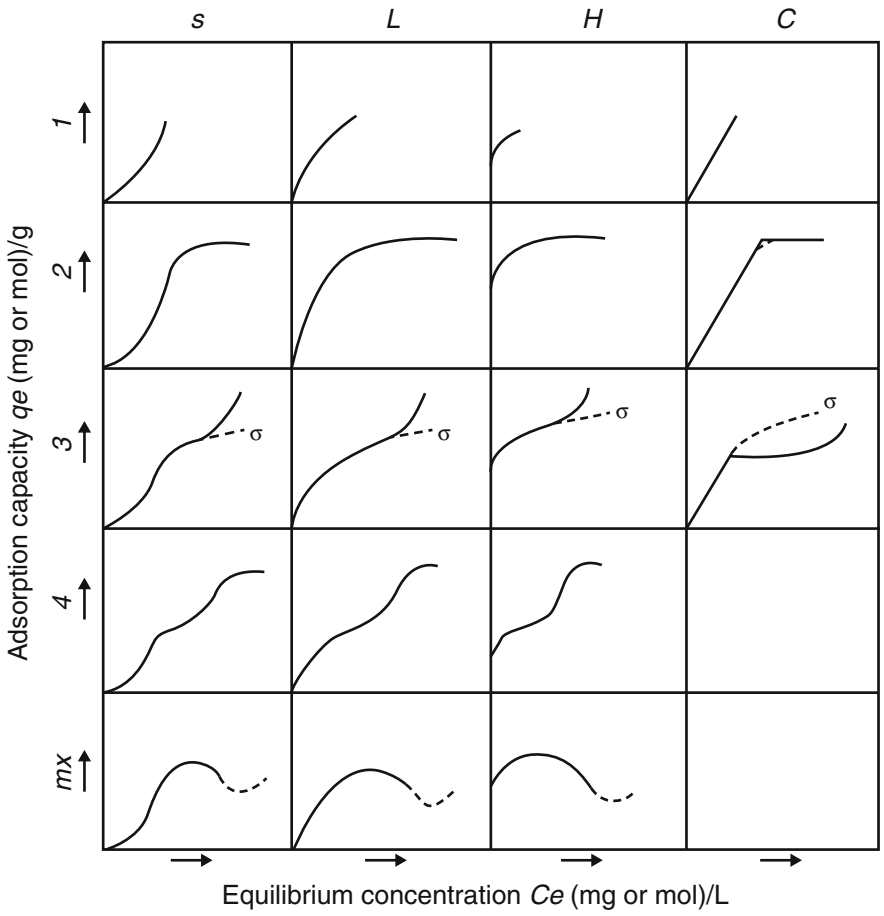

Fig. 2.3 Adsorption isotherm classification (Giles et al. 1960)

to the initial slope into four main classes, and subgroups are described for each class, based on the shapes of the upper parts and slope changes. Figure 2.3 shows the classification proposed by Giles et al. (1960).

The main classes are (i) S curves or vertical orientation isotherm, (ii) L curves or normal or "Langmuir" isotherms, (iii) H curves or high affinity isotherms, and (iv) C curves or constant partition isotherm.

S Curves As can be seen in Fig. 2.3, the S type isotherm has an inclined slope of the curve followed by a vertical orientation. Initially, when the adsorbate concentration increases, there is a chance of the adsorbate to find an available site so that it can occupy, due to competition between solute molecules. Thus, the adsorption capacity is "limited," reaching a plateau. However, this behavior in type S isotherms is opposed, causing the increase of curve slope. This is due to a vertical orientation tendency of the solute molecules in a higher concentration, and then more sites are

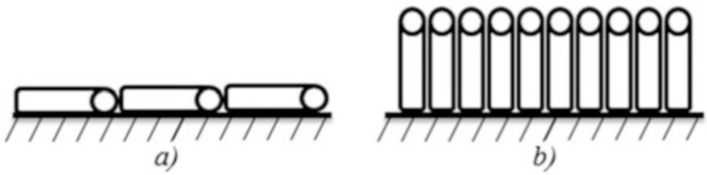

Fig. 2.4 Schematic representation of the molecule orientation in S type isotherms: (**a**) at low concentration; (**b**) at high concentration (Giles et al. 1960)

available for adsorption. In practice, the S curve usually appears when three conditions are fulfilled: (a) the solute molecule is monofunctional; (b) there is a moderate intermolecular attraction, leading to pack vertically in regular array in the adsorbed layer; and (c) there is strong competition, for substrate sites, from molecules of the solvent or another adsorbed species. Figure 2.4 shows a schematic representation of the orientation of the molecules in S type isotherms.

L Curves The normal or Langmuir isotherms are most commonly found in solute adsorption in aqueous solution. The initial shape of the equilibrium curve follows the basic premise that the higher the solute concentration, the greater the adsorption capacity until the number of adsorption site clearance is limited, occurring competition between solute molecules for the available sites. Usually, it is an indicative that the molecules are adsorbed flat on the surface or, sometimes, of vertically oriented adsorbed ions with particularly strong intermolecular attraction. Thus they have one of the following characteristics: (i) the adsorbed molecules are more likely to be adsorbed flat or (ii) are systems with high polar solute and substrate. This isotherm type indicated that the adsorption occurs due to relatively weak forces, such as van der Waals forces.

H Curves The basic difference between the normal isotherms or L type with the high affinity isotherm relates to the beginning of the equilibrium curve. While L type isotherm has its beginning in the origin, H type isotherm shows an initial portion with a vertical orientation, and q_e values are higher than zero, even when the concentration of solute tends to values close to zero. The adsorbed species are often large units, for example, ionic micelles or polymeric molecules However, sometimes, they can be simple ions, which exchange with others of much lower affinity with adsorbent surface, for example, sulfonated dye. This isotherm type indicates chemisorption and adsorption by electrostatic forces. Other classifications commonly used for H type isotherms are like an irreversible isotherm, because when an adsorption occurs at a high concentration, a concentration reduction does not change the adsorption capacity.

C Curves The isotherms with partition constant are characterized by a linear behavior of the equilibrium data at low concentrations of solute. This behavior follows Henry's law for ideal gas equilibrium phases, which translated to adsorption processes, and suggests that the adsorption capacity is proportional to the solute concentration, up until the maximum possible adsorption, where an abrupt

change to a horizontal plateau occurs. This is the type of curve obtained for the partition of a solute between two practically immiscible solvents. In such cases, the affinity of the solute by the solid is greater than the affinity for the solvent, or when the adsorption sites are available in quantities sufficient for the adsorption of all solute, but the bonding forces between the solute and the solvent are weak and depend on the liquid phase concentration.

2.3.1 Subclasses

The subclass 1 of S type isotherm indicates a complete vertical behavior of the adsorption capacity, possibly caused by surface precipitation of solute on the surface of the adsorbent. In the case of classes L, H, and C, they occur when the adsorption sites were not fully occupied, or there was not a complete vertical orientation of the molecules of the solvent. This isotherm type is usually described by the Freundlich model (for the case of L and H type) or Henry's law (for the C type).

The subclass 2 indicates that there is no intermolecular interaction between the solute, forming a long plateau, indicating a saturation of the adsorbent monolayer. In this case, a high energy barrier should be overcome before the additional adsorption can occur on new sites, after the surface has been saturated to the first degree. Therefore, the solute has high affinity for the solvent, but low affinity for the layer of solute molecules already adsorbed. In this case, equilibrium data can be represented by Langmuir model and the plateau is represented by the maximum adsorption capacity (q_m) (for the case of L and H isotherm type).

In subclass 3, a short plateau must mean that the adsorbed solute molecules expose a surface, which has nearly the same affinity for more solute as the original surface possessed. This indicates that the solute in the solution has some intermolecular interaction with the solute in the adsorbent surface, leading to the formation of multilayers.

The subclasses 4 are attributed to the development of a fresh surface in which adsorption can occur. The second plateau represents the complete saturation of the new surface. This additional layer may occur when (i) a proportion of the original surface may be uncovered by reorientation of the molecules already adsorbed, due to intermolecular interactions, (ii) formation of new surfaces in crystalline solids, generating new adsorption sites, or (iii) already exposed parts that allow the formation of two layers, for example, due to formation of micelles.

Finally, the *mx* subclass occurs occasionally when a fall in slope occurs after the first inflection. This is probably due to the association of the solutes in solution; with increase in concentration, the solute–solute attraction begins to increase more rapidly than the adsorbent–solute attraction.

2.4 Adsorption Isotherm Models

2.4.1 Henry's Law

Henry's law can be applied for the adsorption on a uniform surface at sufficiently low concentrations, in which all molecules are isolated from their nearest neighbors. The relationship between the fluid phase concentration and the adsorbed phase equilibrium concentration is linear, with a constant of proportionality, which is equal to the adsorption equilibrium constant, known as the Henry constant (K_H). This linear relationship is commonly referred to as Henry's law by analogy with the limiting behavior of dissolution of gases in liquids. The constant of proportionality, which is simply the adsorption equilibrium constant, is referred to as the Henry constant (K_H) and may be expressed in terms of concentration:

$$q_e = K_H C_e \tag{2.10}$$

For physical adsorption, there is no change in molecular state of adsorption, i.e., for adsorption on a uniform surface at sufficiently low concentration, all molecules are isolated from their nearest neighbors. The equilibrium relationship between fluid phase and adsorbed phase concentration will be linear, and the relation to the surface concentration (n_s) can be presented in Eq. (2.11):

$$n_s = \frac{K_H}{a} C_e \tag{2.11}$$

where a is the specific surface area per unit volume of the adsorbate (Ruthven 1984).

2.4.2 Monolayer Adsorption and the Langmuir Isotherm

The adsorbent and the adsorbate are in dynamic equilibrium, and the fractional coverage of the surface depends on the concentration of the adsorbate. The extent of surface coverage is normally expressed as the fractional coverage, θ (Langmuir 1918):

$$\theta = \frac{\text{Number of adsorption sites occupied}}{\text{Number of adsorption sites available}} \tag{2.12}$$

The physical simplicity of the isotherm is based on four assumptions (Atkins and De Paula 2006):

- Adsorption cannot occur beyond monolayer coverage.
- Each site can hold only one adsorbate molecule.

- All sites are energetically equivalent and the surface is uniform.
- The ability of a molecule to adsorb in a given site is independent of the occupation of neighboring.

In the dynamic adsorption equilibrium, the adsorption and desorption rates are the same, so

$$A(\text{aq}) + M(\text{surface}) \Leftrightarrow AM(\text{surface}) \tag{2.13}$$

The rate of surface coverage due to adsorption is proportional to the solution concentration C_A of A and the number of vacant sites $N(1-\theta)$, where N is the total number of sites and can be expressed as

$$\frac{d\theta}{dt} = k_a C_\text{A} N(1-\theta) \tag{2.14}$$

The change of θ due to desorption is proportional to the number of adsorbed species $N\theta$, so

$$\frac{d\theta}{dt} = -k_d N\theta \tag{2.15}$$

where the kinetic constants are k_a for adsorption and k_d for desorption.

At equilibrium, there is no change in the composition in both phases (the sum of these two rates is equal to zero), and solving for θ results in the Langmuir isotherm:

$$\theta = \frac{K_\text{L} C_e}{1 + K_\text{L} C_e} \tag{2.16}$$

where the Langmuir constant (K_L) is

$$K_\text{L} = \frac{k_a}{k_d} \tag{2.17}$$

Considering the exchange of molecules between adsorbed and liquid phase, the fraction covered can be considered the relation between the adsorption capacity at equilibrium (q_e) and the maximum adsorption capacity, which occur when all sites of the monolayer are occupied (q_m).

$$\theta = \frac{q_e}{q_m} \tag{2.18}$$

Replacing Eq. (2.18) in Eq. (2.16), the Langmuir equation becomes

$$q_e = \frac{q_m k_\text{L} C_e}{1 + k_\text{L} C_e} \tag{2.19}$$

2.4.3 Multilayer Adsorption and the BET Isotherm

When the initial adsorbed layer becomes a surface for further adsorption, instead of the isotherm stabilized in a saturated monolayer, the formation of multilayers can be expected. The most widely used isotherm for the multilayer adsorption was derived by Brunauer et al. (1938) and is called the BET isotherm. In liquid systems, the BET isotherm is (Ebadi et al. 2009)

$$q_e = \frac{q_{\mathrm{BET}} k_1 C_e}{(1 - k_2 C_e)(1 - k_2 C_e + k_1 C_e)} \tag{2.20}$$

where q_{BET} is the monolayer adsorption capacity (mg/g), k_1 and k_2 are the BET constants (L/mg).

2.4.4 Other Isotherm Models

In the Langmuir isotherm model, the independence and energetic equivalence of the adsorption sites are attributed. Deviations of this supposition can be identified using other models. Various attempts have been made to take these variations into account.

2.4.4.1 Temkin Isotherm

The Temkin isotherm equation assumes that the heat of adsorption of all the molecules in the layer decreases linearly with coverage due to adsorbent–adsorbate interactions and that the adsorption is characterized by a uniform distribution of the binding energies, up to some maximum binding energy. The Temkin model is given by

$$\theta = \frac{RT}{\Delta Q} \ln (K_{\mathrm{T}} C_e) \tag{2.21}$$

where θ is the fractional coverage (defined in Eq. 2.17), R is the universal gas constant (kJ/mol K), T is the temperature (K), $\Delta Q = -\Delta H$ is the variation of adsorption energy (kJ/mol), and K_{T} is the Temkin equilibrium constant (L/mg).

2.4.4.2 Freundlich Isotherm

The Freundlich isotherm assumes that the adsorption occurs on a heterogeneous surface, and the amount that is adsorbed increases infinitely with an increase in concentration (Freundlich 1906). In liquid phase, this isotherm is given by

$$q_e = k_F C_e^{1/n_F} \tag{2.22}$$

where k_F is the Freundlich constant (a common error is noted in k_F unit, i.e., mg^{1-c} L^c/g, where $c = 1/n_F$) and $1/n_F$ is the heterogeneity factor. This isotherm attempts to incorporate the role of adsorbate–adsorbate interactions on the surface.

2.4.4.3 Dubinin–Radushkevich (D-R) Isotherm

The Dubinin–Radushkevich (D-R) isotherm model considers that adsorbent size is comparable to the micropore size, and the adsorption equilibrium relation for a given adsorbate–adsorbent combination can be expressed independently of temperature by using the adsorption potential (ε), according to Eq. (2.23):

$$\varepsilon = RT \ln\left(1 + \frac{1}{C_e}\right) \tag{2.23}$$

The D-R isotherm assumes a Gaussian-type distribution for the characteristic curve and the model can be described by Eq. (2.24):

$$q_e = q_{max} \exp\left(-\beta \varepsilon^2\right) \tag{2.24}$$

where q_{max} is the D-R constant (mg/g) and β gives the mean sorption free energy E (kJ/mol) at the moment of its transfer to the solid surface from the bulk solution and can be computed using Eq. (2.25):

$$E = \frac{1}{(2\beta)^{1/2}} \tag{2.25}$$

2.4.4.4 Redlich–Peterson (R-P) Model

The Redlich and Peterson (1959) developed an empirical isotherm model at three parameters used to represent the adsorption equilibrium over a wide concentration range and can be applied in either homogeneous or heterogeneous systems due to its versatility. The R-P model combines elements of Langmuir and Freundlich models and is shown in Eq. (2.26):

$$q_e = \frac{k_R C_e}{1 + a_R C_e^{\beta}} \tag{2.26}$$

where k_R and a_R are the R-P constant (L/g and L^{β}/mg^{β}, respectively) and β is the exponent, which can vary between 1 and 0.

Besides the R-P model, a number of other isotherm models of three and four parameters were developed empirically. However, most are simple modifications of Langmuir and Freundlich models, without a significant relevance in adsorption studies.

2.4.5 Statistical Physics Models

Some models based on statistical physics are used to fit and interpret the adsorption isotherms in liquid phase. The hypotheses of the statistical physics models are more complicated and are developed by using the canonical ensemble in statistical physics. Consequently, the interpretations of the adsorption process using the statistical physics models are more useful. The statistical physics models have physicochemical parameters, which are able to explain the adsorption from the macroscopic and microscopic viewpoints.

The statistical physics models suppose that a variable number of ions/molecules are adsorbed on N_M receptor sites per unit surface (identical receptor sites) and independent receptor sites (N_{M1} and N_{M2}) of the adsorbent surface. To establish the statistical physics models, it is necessary to write the expression of the partition function of one receptor site. The general expression is given by

$$Z_{gc} = \sum_{N_i=0,1\ldots} e^{-\beta(-\varepsilon_i-\mu)N_i} \tag{2.27}$$

where $(-\varepsilon_i)$ is the adsorption energy of receptor site, μ is the chemical potential of receptor site, N_i is the occupation state of receptor site, and β is defined as $1/k_B T$ (where k_B is the Boltzmann constant and T the absolute temperature).

If the receptor sites are identically related to N_M receptor sites, the total grand canonical partition function is written as

$$Z_{gc} = \left(z_{gc}\right)^{N_M} \tag{2.28}$$

But, if the receptor sites are independent (two types of receptor sites), the total grand canonical partition function is given by

$$Z_{gc} = \left(z_{gc_1}\right)^{N_{M1}} \left(z_{gc_2}\right)^{N_{M2}} \tag{2.29}$$

According to the literature, the average site occupation number N_o can be written as

$$N_o = k_B T \frac{\partial \ln Z_{gc}}{\partial \mu} \tag{2.30}$$

When the thermodynamic equilibrium is reached, the equality between the chemical potentials can be written as $\mu_m = \mu/n$ where μ is the chemical potential

of the adsorbed ions/molecules, n is the number or fraction of ions/molecules per site, and μ_m is the chemical potential of dissolved ions/molecules as

$$\mu_m = k_B T \ln\left(\frac{N}{z_{tr}}\right) \tag{2.31}$$

where z_{tr} is the translation partition function, according to

$$z_{tr} = V\left(\frac{2\pi m k_B T}{h^2}\right)^{3/2} \tag{2.32}$$

where m is the adsorbed mass, h is the Planck constant, and V is the volume of studied system. Finally, the adsorbed quantity as function of concentration describing the expression of the statistical physics model is given by

$$Q = nN_0 \tag{2.33}$$

By the application of the general methodology describing the statistical physics model development, the expressions of the discussed models are presented in Table 2.1.

2.4.6 *Typical Values of Isotherm Parameters for Different Adsorbate–Adsorbent Systems*

Table 2.2 presents typical values of the parameters of the isotherm models for different adsorption systems in liquid phase. Henry's law is applied to represent C1 isotherm type, according to Giles et al. (1960) classification, when the number of

Table 2.1 Statistical physics models based on the general partition function

Model	Equation	
Monolayer model with one energy	$Q = \dfrac{Q_0}{1+\left(\dfrac{c_{1/2}}{c}\right)^n}$	(2.34)
Monolayer model with two energies	$Q = \dfrac{n_1 N_{1M}}{1+\left(\dfrac{c_1}{c}\right)^{n_1}} + \dfrac{n_2 N_{2M}}{1+\left(\dfrac{c_2}{c}\right)^{n_2}}$	(2.35)
Double layer model with two energies	$Q = nN_M \dfrac{\left(\dfrac{c}{c_1}\right)^n + 2\left(\dfrac{c}{c_2}\right)^{2n}}{1+\left(\dfrac{c}{c_1}\right)^n + \left(\dfrac{c}{c_2}\right)^{2n}}$	(2.36)
Multilayer model with saturation	$Q = nN_M \dfrac{[F_1(c)+F_2(c)+F_3(c)+F_4(c)]}{[G(c)]}$	(2.37)

Table 2.2 Isotherm parameters for several adsorbent–adsorbate systems

Adsorbent	Adsorbate	Parameters		References
Henry law		k_H (L/g)		
Fungal biomass	Acid yellow 49	0.848		Russo et al. (2010)
Chromium tanned leather waste	Acid yellow 194	1.909		Piccin et al. (2013)
Calcined diatomite	Methylene Blue	0.26		Khraisheh et al. (2005)
	Reactive black	0.36		
	Reactive yellow	0.17		
Diatomaceous earth	Reactive black	0.42		Al-Ghouti et al. (2003)
	Reactive yellow	0.18		
Langmuir model		k_L (L/mg)	q_m (mg/g)	
Sugarcane bagasse	Ni(II)	0.173	64.1	Dotto et al. (2016b)
Chitosan/bentonite composite	Methylene Blue	2.055	496.5	Dotto et al. (2016c)
Chitosan	FD&C red 40	0.395	372.9	Piccin et al. (2009)
Papaya seeds	Tartrazine	0.373	51.0	Weber et al. (2014)
Fungal biomass	Acid blue 62	0.024	300	Russo et al. (2010)
Natural palygorskite	Methylene Blue	0.010	187.3	Zhang et al. (2015)
S. melongena leaf powder	Pb(II)	0.274	71.4	Yuvaraja et al. (2014)
$CoFe_2O_4$ graphene oxide	Pb(II)	0.095	299.4	Zhang et al. (2014)
	Hg(II)	0.237	157.9	
Activated carbon	Lanaset gray G	0.208	108.7	Baccar et al. (2010)
Activated carbon	Anthracene	0.260	8.35	Saad et al. (2014)
Activated carbon	Fluoxetine	0.375	1112.0	Nabais et al. (2008)
Freundlich model		k_F ($mg^{1-c}L^c/g$)	n_F	
Ca-bentonite	Congo red	26.91	3.23	Lian et al. (2009)
Dried soya bean meal	Reactive red 2	5.268	1.079	Sahadevan et al. (2009)
NKA-2 resin	Flavones	23.11	1.789	Chen and Zhang (2014)
Fe_3O_4 nanospheres	Neural red	10.62	2.17	Iram et al. (2010)

Activated carbon	Polyphenols	6787.97		0.112	Marsal et al. (2009)
Acid-treated oil shale ash	Deltamethrin	2.406		2.01	Al-Qodah et al. (2007)
Cationic polymer-loaded bentonite	Acid scarlet GR	15.35		4.484	Li et al. (2010)
	Acid dark blue 2G	20.58		5.319	
Cashew nut shell	Congo red	1.357		2.279	Kumar et al. (2010)
Cationic polymer/bentonite	Acid dark blue 2G	12.834		4.47	Qian Li et al. (2010)
Fungal biomass	Acid red 266	114		3.7	Russo et al. (2010)
Temkin model		k_T (L/g)		ΔQ (J/mol)	
Activated carbon from waste biomass	Methylene Blue	33.8		1307	Nunes et al. (2009)
Zeolites	Phenol	16.7		537.6	Yousef et al. (2011)
Surface modified tannery waste	Rhodamine B	1.04		69.9	Anandkumar and Mandal (2011)
	Cr (VI)	7.06		117.3	
BET model		k_1 (L/mg)	k_2 (L/mg)	q_{BET} (mg/g)	
Perfluorooctyl alumina	MTBE	1.2251×10^{-2}	4.6965×10^{-4}	3.5	Ebadi et al. (2007)
Chitosan films	Vanadium	1.3×10^{-2}	2.97×10^{-3}	90.13	Cadaval et al. (2016)
Formaldehyde-pretreated *Pinus pinaster* bark	Phenol	37.84	6.19×10^{-2}	0.086	Vázquez et al. (2007)
Chromium-tanned leather waste	Acid black 210	0.522	1.7×10^{-3}	108.8	Piccin et al. (2013)
Carbonized bark	Pentachlorophenol	16.224	0.184	0.841	Ebadi et al. (2009)[a]
RP model		k_R (L/mg)	α_R (L^{β}/mg^{β})	β	
Cashew nut shell	Congo red	5.548	3.186	0.638	Kumar et al. (2010)
Zeolites	Phenol	51.5	6.28	0.72	Yousef et al. (2011)

[a]Using data of Edgehill (1998)

adsorption sites is very superior to the number of adsorbate molecules, due to a hydrophobic interaction between the adsorbent and adsorbate. The increase of k_H constant represents an increase of adsorption capacity at low concentrations.

The Langmuir model is satisfactory to represent H2 or L2 isotherm type, according to Giles et al. (1960) classification. In practice, the constant k_L is associated with increased affinity of the adsorbate by adsorbent, since k_L represents the inverse of the equilibrium concentration in the liquid phase when the adsorption capacity reaches 50% of the monolayer adsorption capacity (or $f(1/k_L) = 0.5q_m$, where f is the function of the Langmuir isotherm). Therefore, k_L increase leads to a higher initial slope of the adsorption isotherm. On the other hand, q_m is associated with the curve plateau formation and complete saturation of the monolayer adsorbate. q_m is in the order from unity to tens of milligrams per gram in the case of monatomic ion adsorption and in the order from hundreds to thousands of milligrams per gram for dyes and larger molecule adsorption. However, Table 2.2 shows that the maximum monolayer adsorption capacity can vary due to many factors, such as chemical structure of the adsorbate and adsorbent, molecular size, and nature of the adsorbent.

The Freundlich model is satisfactory to describe the adsorption isotherm data of types S, L, and C (subclass 1). The $0 < n_F < 1$ when the isotherm is of class S (or unfavorable), $n_F > 1$ when the isotherm is of class L (or favorable), and $n_F = 1$ when the isotherm is of class C. In the latter case, usually when the number of adsorption sites is greater than the number of molecules to be adsorbed, the Freundlich model is simplified to Henry model. Already, the k_F values are associated with the initial slope of the isotherm curve.

The BET isotherm is an extension of the Langmuir theory for monolayer adsorption to multilayer adsorption, and it is satisfactory to represent the H3 or L3 isotherm type, according to the Giles et al. (1960) classification. q_{BET} and k_1 have the same physical significance as to that of q_m and k_L Langmuir constant, respectively.

Then, an increase in the equilibrium concentration leads to an increase of adsorption capacity. This behavior is due to secondary adsorption at a given site, forming a multilayer and providing a suitable adjustment to the BET model. The multilayer formation may occur due to a change in organizational form of dye molecules arranged on the surface of the adsorbent, in horizontal to vertical alignment, or due to solubility reduction caused by superficial hydrophobic interactions between the adsorbate and the adsorbent (Piccin et al. 2013). The k_2 constant represents the inverse of the concentration value when the isotherm becomes a vertical line and is associated with superficial solubility of adsorbate ($C_s = 1/k_2$). The k_2 value increment is due to a vertical orientation of the isotherm at lower equilibrium concentration in the liquid phase. In this case, Ebadi et al. (2009) demonstrated that the use of adsorbent solubility concentration leads to serious errors in the interpretation of the adsorption data. According to the authors, k_2 or C_s must be obtained by adjusting the model to experimental data. When k_2 tend to

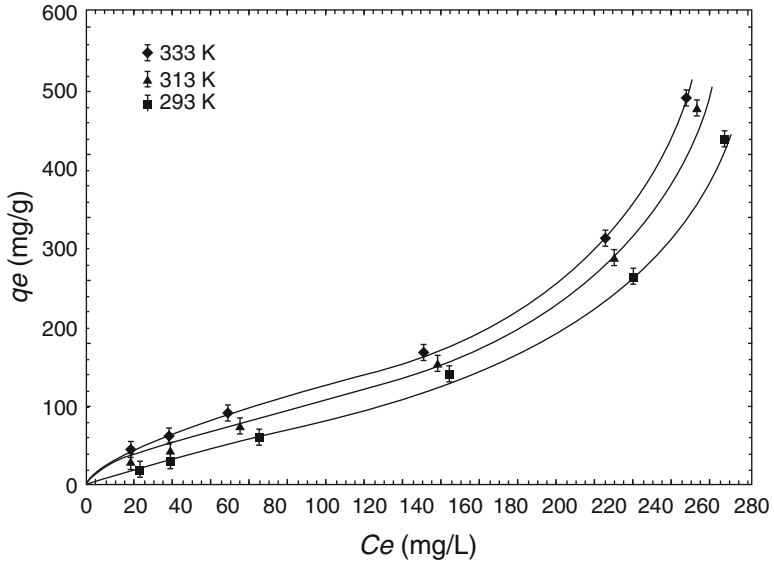

Fig. 2.5 Equilibrium isotherms following the BET multilayer model for vanadium adsorption onto chitosan films (Cadaval et al. 2016)

zero, the BET model can be mathematically simplified to the Langmuir model, releasing degrees of freedom for the model and simplifying the use of the data (Piccin et al. 2013).

Figure 2.5 shows the equilibrium curves of vanadium adsorption onto chitosan films at different temperatures (Cadaval et al. 2016). In this example, the temperature increase led to an increase in the q_{BET} value from 90.9 to 102.3 mg/g. This behavior suggests an endothermic phenomenon. The k_1 and k_2 values increased with increasing temperature. The k_1 increase indicates that lower equilibrium concentrations are necessary to saturate the monolayer, and the k_2 increase indicates that smaller equilibrium concentrations are necessary to the isotherm that becomes a vertical line. However, Piccin et al. (2013) observed contrary behavior toward the concentration of surface saturation (C_s). In this case, a temperature reduction led to a reduction of C_s values, indicating that the highest adsorption capacities by multilayer formation were obtained with lower equilibrium concentrations. This reduction is associated with the solubility of the dye in water, generally lower at high temperatures, and the increased adsorbate–absorbent forces at low temperatures.

Regarding the Redlich–Peterson model, and other models of three and four parameters reported in the literature (Wong et al. 2004; Piccin et al. 2009; Kumar et al. 2010; Yousef et al. 2011), in most cases these do not provide suitable adjustments to the experimental data to the point of its use to be justified. In this case, simpler models such as Langmuir or Freundlich are satisfactory to represent the experimental data.

2.5 Regression Methods and Error Analysis

Several models are able to describe the experimental results of adsorption and are used in equilibrium, kinetics, and mechanisms studies. In the process of statistically analyzing empiric data, errors that lead to the unreliable results can occur. The misuse of linearization is a common error in data analysis. When the data are transformed in order to achieve a linear equation, it is required to know how the error-structure of the data is affected by this tranformation. When the errors are additive on the dependent variable and the usual assumptions of normality and equal variance throughout the range of the data are checked, then the transformation of the dependent variable with a nonlinear function can eliminate the distributional properties. This can occur in the linearization of adsorption isotherms; for example, the Langmuir model (Eq. 2.19) is nonlinear; thus the dependent variable does not depend linearly on the independent variable (El-Khaiary and Malash 2011).

These nonlinear forms can be mathematically manipulated and linearized at different linear forms. Moreover, the statistical tests used to check the fit will often not detect that the parameters are biased. Table 2.3 presents the different linearizations to the Langmuir and Freundlich models.

The statistical regression methods consist in minimizing objective functions through the variation of the model parameters. Table 2.4 summarizes some of these functions and its main characteristics.

From Eqs. (2.42), (2.43), and (2.44), *SSE*, R^2, and *ABS* provide a better fit for higher y_{exp} values, because errors are proportional to their magnitudes. *SSE* is the most common error function in use. In the R^2 function, the objective is to maximize the results, and the *ABS* is similar to the *SSE* to some extent. In relation to Eqs. (2.45), (2.46), (2.47), and (2.48), the values of (χ^2), *ARE*, *HYBRID*, and *MPSD* improve the fit at low concentrations by dividing by the experimental value *HYBRID*, and *MPSD* also includes the number of degrees of freedom of the system, which is important in the analysis of models with different parameter numbers.

The main objective function used for both linear and nonlinear regressions is the sum of the squares of the errors (SSE). In the case of linearized forms of the Langmuir model, the function $y = \beta_0 + \beta_1 \cdot x$ represents the experimental data.

Table 2.3 Linearized form of adsorption isotherm models

Model	Linearized form	Plot	
Langmuir I	$\frac{C_e}{q_e} = \frac{1}{k_L q_m} + \frac{1}{q_m} C_e$	$\frac{C_e}{q_e}$ vs. C_e	(2.38)
Langmuir II	$\frac{1}{q_e} = \frac{1}{q_m} + \frac{1}{k_L q_m C_e}$	$\frac{1}{q_e}$ vs. $\frac{1}{C_e}$	(2.39)
Langmuir III	$\frac{q_e}{C_e} = k_L q_m + k_L q_e$	$\frac{q_e}{C_e}$ vs. q_e	(2.40)
Freundlich	$\log(q_e) = \log(k_F) + \frac{1}{n_F} \log(C_e)$	$\log\ (q_e)$ vs. $\log\ (C_e)$	(2.41)

Table 2.4 Error function used for isotherm model regression

Function name	Error function	
Sum of square error (SSE)	$\mathrm{SSE} = \sum_{i=1}^{n} \left(y_{i,\mathrm{exp}} - y_{i,\mathrm{mod}}\right)^2$	(2.42)
Coefficient of determination (R^2)	$R^2 = 1 - \dfrac{\sum_{i=1}^{n} \left(y_{i,\mathrm{exp}} - y_{i,\mathrm{mod}}\right)^2}{\sum_{i=1}^{n} \left(y_{i,\mathrm{exp}} - \overline{y_{i,\mathrm{exp}}}\right)^2} = 1 - \dfrac{\mathrm{SSE}}{\mathrm{SST}}$	(2.43)
Sum of the absolute errors (ABS)	$\mathrm{ABS} = \sum_{i=1}^{n} \left\lvert y_{i,\mathrm{exp}} - y_{i,\mathrm{mod}} \right\rvert$	(2.44)
Chi-square (χ^2)	$\chi^2 = \sum_{i=1}^{n} \dfrac{\left(y_{i,\mathrm{exp}} - y_{i,\mathrm{mod}}\right)^2}{y_{i,\mathrm{mod}}}$	(2.45)
Average relative error (ARE)	$\mathrm{ARE} = \dfrac{100}{n} \sum_{i=1}^{n} \left\lvert \dfrac{y_{i,\mathrm{exp}} - y_{i,\mathrm{mod}}}{y_{i,\mathrm{mod}}} \right\rvert$	(2.46)
Hybrid fractional error function (HYBRID)	$\mathrm{HYBRID} = \dfrac{100}{n - n_p} \sum_{i=1}^{n} \dfrac{\left(y_{i,\mathrm{exp}} - y_{i,\mathrm{mod}}\right)^2}{y_{i,\mathrm{mod}}}$	(2.47)
Marquardt's percent standard deviation (MPSD)	$\mathrm{MPSD} = 100 \sqrt{\dfrac{1}{n - n_p} \sum_{i=1}^{n} \left[\dfrac{\left(y_{i,\mathrm{exp}} - y_{i,\mathrm{mod}}\right)}{y_{i,\mathrm{mod}}} \right]^2}$	(2.48)

Where $y_{i,\,\mathrm{exp.}}$ is the experimental value of independent variable, $y_{i,\,\mathrm{mod}}$ is the modeled value, $\overline{y_{\mathrm{exp}}}$ is the mean of observed values, *SST* is the sum of squares of total deviations, n is the number total of informations, and n_p is the number of parameters of the model

Thus, β_0 and β_1 values can be obtained from the minimization of the objective function (SSE) using the method of linear least squares estimation. However, for nonlinear form of the isotherm models, there is no closed method for obtaining parameters. Instead, in this case, numerical algorithms are used to minimize the objective function and obtain the values of the model parameters. Most algorithms involve choosing initial values for the parameters. Then, the parameters are refined iteratively, that is, the values are obtained by successive approximation. The most commonly used algorithms, in this case, are the Gauss–Newton, Levenberg–Marquardt and the Generalized Reduced Gradient.

2.5.1 Model Accuracy

The coefficient of determination (R^2), defined above, to obtain the more suitable model to represent equilibrium and kinetic and thermodynamic parameters is another common practice in adsorption experiments.

The R^2 value is very sensitive to extreme data points, resulting in misleading indication of the fit. The R^2 is also influenced by the range of the independent

variable and increases as the range of independent variable increases and decreases as the range decreases. These issues can be avoided by fitting the data to the model without any transformations and by examination of extreme points.

Another relevant fact is that the R^2 can be made manipulated using more parameters in the model, since the increase in the number of regression parameters leads to decreases in *SSE* value. Therefore, the good fit cannot be based only on *SSE* (and R^2). This is especially common in adsorption studies when it comes to estimating equilibrium parameters. For this fact, the analysis of the adjusted determination coefficient ($R_{adj}{}^2$), which takes into account the experimental degrees of freedom ($n-1$) and the model degrees of freedom ($n-(n_p + 1)$), can be a good tool in selecting models. $R_{adj}{}^2$ is described in Eq. (2.49):

$$R_{adj}{}^2 = 1 - \left(\frac{n-1}{1-(n_p+1)}\right)(1+R^2) \tag{2.49}$$

where n is the number of information and n_p is the number of model parameters.

Moreover, Akaike's information criterion (AIC) (Anderson and Burnham 2002) is a well-established statistical method that can be used to compare the models with different numbers or parameters. For a small sample size, AIC is calculated for each model from Eq. (2.50):

$$\mathrm{AIC} = n\ln\left(\frac{\mathrm{SSE}}{n}\right) + 2n_p + \frac{2n_p(n_p+1)}{n-(n_p+1)} \tag{2.50}$$

A smaller AIC value suggests that the model has more likely to show a better fit. The AIC values can be compared using the evidence ratio (Er), which is defined by

$$\mathrm{Er} = \frac{1}{e^{-0.5\Delta}} \tag{2.51}$$

where Δ is the absolute value of the difference in AIC between the two models. The evidence ratio means how many times one model is more likely than the other one in relation to the experimental data.

2.5.2 Comparison Between Linear and Nonlinear Regression Methods

In this section, we want to show the effect of the regression method used on the parameters of the model and the adjustment to the experimental data. To exemplify this, we use common adsorption data of a FD&C Red No. 40 dye onto chitosan with deacetylation degree of 84%, particle size of 99 μm, and pH 7.0 at 25 °C (Piccin et al. 2009). The model parameters were obtained by the different linearized forms

of models (Table 2.5), using the linear least squares estimation method, and by the nonlinear models (Eqs. (2.19), (2.20), (2.21), and (2.22)), using GRG nonlinear algorithm of add-in solver function of MS Excel (Microsoft, USA). Figure 2.6 shows the experimental data. Figure 2.7 shows the linearized data according to Langmuir I, II, and III and Freundlich forms, respectively.

According to Fig. 2.7d, the linearized form of Freundlich model shows a best fit ($R^2 = 0.9797$). However, the forms I and III of Langmuir model have poor adjustment ($R^2 < 0.900$) to the experimental data. However, in Table 2.5, it can be observed that the R^2 and SSE values for Langmuir, independent of the way of obtaining the model parameters, provide a better fit to the experimental data. These data make it clear that the different forms of linearization can lead to serious errors

Table 2.5 Model parameters and respective determination coefficient (R^2) and sum of square error (SSE) from adsorption of acid red No. 40 onto chitosan obtained by different regression methods

Model	Parameters			
Langmuir	$k_L \times 10^3$ (L/mg)	q_m (mg/g)	R^2	SSE
Nonlinearized	4.656	181.6	0.9918	174.41
Langmuir I	4.121	193.6	0.9911	188.63
Langmuir II	2.659	269.4	0.9684	675.36
Langmuir III	3.739	207.4	0.9899	218.65
Freundlich	k_F (mg^{1-c} L^c/g)	n_F	R^2	SSE
Nonlinearized	2.896	1.559	0.9821	383.44
Linearized	1.659	1.328	0.9690	662.51

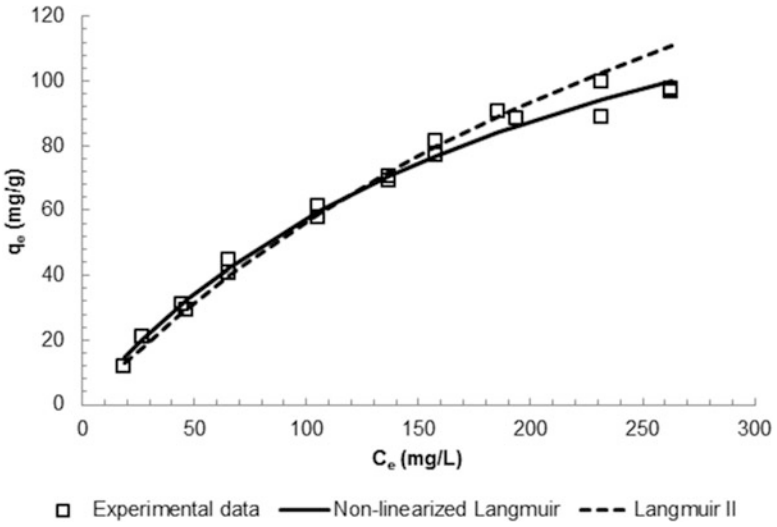

Fig. 2.6 Adsorption equilibrium data of acid red No. 40 dye by chitosan (Piccin et al. 2009)

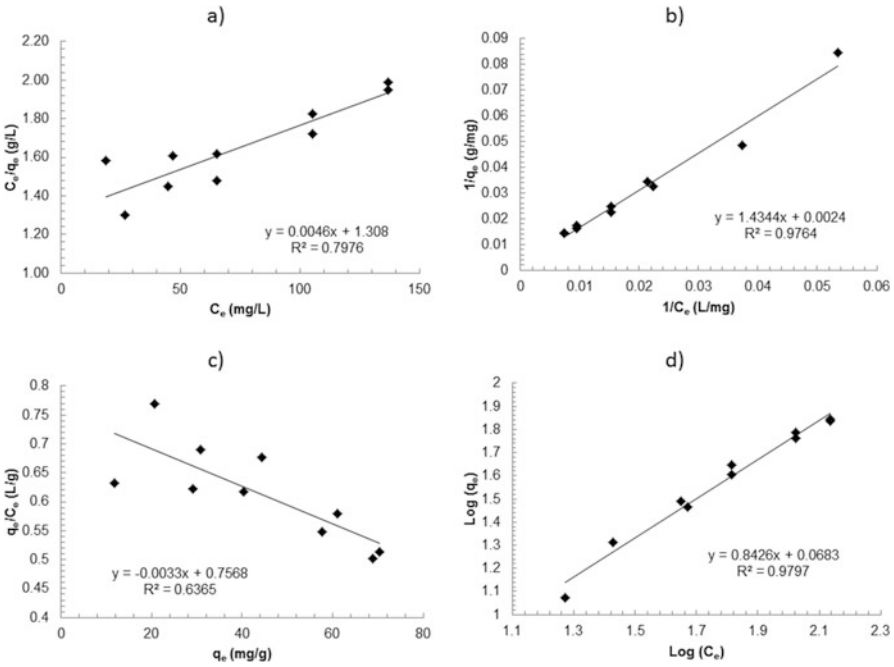

Fig. 2.7 Adjustment of the linearized forms of models to equilibrium experimental data of FD&C red No. 40 dye onto chitosan: (**a**) Langmuir I; (**b**) Langmuir II; (**c**) Langmuir III; and (**d**) Freundlich

in the conclusion of which model is most suitable to represent the experimental data. The use of one variable both as dependent and independent variable, as in the case of Langmuir I (C_e) and Langmuir III (q_e), leads to an inadequate correlation. The error distribution of the dependent variable (C_e/q_e or q_e/C_e) is different from both the error distributions of C_e and q_e. In the case of Langmuir II, the reversal of relative weights of data points because of $1/q_e$ and $1/C_e$ in dependent and independent variables, respectively, leads to distortion of error distribution. This distortion can be observed in Fig. 2.7b, where most of the data are grouped together in a small space of the Cartesian plane, near to the origin. For the Freundlich linearized model, an alteration of relative weights of the data because of $\log(q_e)$ in the dependent variable and a distortion of relative weights of data because of $\log(q_e)$ and $\log(C_e)$ in the dependent and independent variables, leading to distortion of error distribution, occur.

Furthermore, it is observed that Langmuir II form, which has best linearized fit, overestimates the q_m values, when compared to the other forms of the model. In this case, the model fit curve introduces distortions of the experimental data for high adsorption capacity, as shown in Fig. 2.7 (solid lines), which can lead to errors in the analysis and design of the equipment. For this reason, the correct form of the analysis and modeling equilibrium curves is through normalized form (or not

linearized) of the equilibrium data. The linearization can be used as a method of visual analysis of the data range to which a model will fit properly to the experimental data (e.g., equilibrium curves with multilayer adsorption), but not as the conclusion about the adjustment of or obtaining the model parameters.

2.6 Adsorption Thermodynamics

In solid–liquid adsorption systems, the estimation of the thermodynamic parameters is essential. In general, the adsorption thermodynamics is studied by the estimation of standard Gibbs free energy change (ΔG^0), standard enthalpy change (ΔH^0), and standard entropy change (ΔS^0) (Crini and Badot 2008). From these parameters, it is possible to verify if the adsorption is favorable, spontaneous, endothermic, or exothermic. It is possible to obtain information regarding the disorder in the solid–liquid interface during the adsorption. Also, it is possible to infer about the adsorption nature, i.e., physisorption or chemisorption, and verify if the operation is controlled by enthalpy or entropy (Ruthven 1984; Dotto et al. 2016a). Indeed, the correct calculation of the adsorption thermodynamic parameters is fundamental.

In the thermodynamic sense, the majority of the studies has considered the adsorption as a reaction (Liu 2009):

$$A + B \longleftrightarrow AB \tag{2.52}$$

The adsorbent (A) interacts with the adsorbate (B), forming AB. When this reaction attains the thermodynamic equilibrium, the chemical potentials in the liquid phase (μ_l) and in the solid–liquid interface (μ_{s-l}) are equal, and the Gibbs free energy change (ΔG) tends to zero, leading to Eq. (2.53) (Chen and Zhang 2014):

$$\Delta G = \mu_{s-l} - \mu_l = \Delta G^0 + RT \ln (K_e) = 0 \tag{2.53}$$

then,

$$\Delta G^0 = -RT \ln (K_e) \tag{2.54}$$

where R is the universal gas constant, T is the temperature, and K_e is the equilibrium thermodynamic constant.

The relationship of ΔG^0 with ΔH^0 and ΔS^0 can be expressed as (Liu 2009)

$$\Delta G^0 = \Delta H^0 - T\Delta S^0 \tag{2.55}$$

Substituting Eq. (2.54) in Eq. (2.55), the following relation is obtained:

$$\ln(K_e) = -\frac{\Delta H^0}{RT} + \frac{\Delta S^0}{R} \tag{2.56}$$

Then, by the plot of $\ln(K_e)$ versus $(1/T)$, the values of ΔH^0 and ΔS^0 can be found. The graph is known as the Van't Hoff plot. This methodology is used in several works in order to estimate the adsorption thermodynamic parameters (Crini and Badot 2008; Dotto et al. 2015a).

The use of Van't Hoff plot is relatively simple but is dependent of the correct calculation of the equilibrium thermodynamic constant K_e. Indeed, the K_e values are calculated by different manners in the literature, and some of these manners are unreasonable (Milonjic 2007). For example, in most cases, K_e is used with units. However, from the mathematical viewpoint, a parameter that has a dimension cannot be computed logarithmically. The parameter in transcendental functions must be dimensionless; otherwise, the computation for this parameter does not make sense (Zhou et al. 2012). In other cases, K_e is obtained from the distribution constant ($K_e = C_{ad}/C_e$) (being C_e and C_{ad}, the adsorbate concentrations in solution and in solid phase at equilibrium, respectively). This is valid only at very low adsorbate concentrations. Another way is the use of the isotherm parameters (e.g., Langmuir, $K_e = \rho q_m K_L$). This is not completely correct but is reasonable, since the initial slope of the isotherm can be compared with the Henry constant K_H (Dotto et al. 2013).

As presented above, the correct calculation of K_e is a discussed topic, without common sense. Here, a reasonable mean to find K_e is presented. In a solid–liquid adsorption system, the equilibrium thermodynamic constant is given by Eq. (2.57) (Liu 2009):

$$K_e = \frac{\text{activity of occupied sites}}{(\text{activity of vacant sites})(\text{activity of adsorbate in solution})} \tag{2.57}$$

Assuming that the activity of the occupied and unoccupied sites is the same, Eq. (2.57) becomes (Zhou et al. 2012)

$$K_e = \frac{\theta}{(1-\theta)\alpha_e} \tag{2.58}$$

where α_e is the activity of the adsorbate in solution at equilibrium and θ is the fraction of the surface covered at equilibrium. For the Langmuir model, θ is given by Eq. (2.18) (for other isotherms, q_m can be replaced by the parameter relative to the maximum adsorption capacity in mol/g). The activity of a substance can be related to its molar concentration (C_e) according to Eq. (2.59) (Smith et al. 2005):

$$\alpha_e = \frac{\gamma_e C_e}{\gamma^0 C^0} \tag{2.59}$$

where γ_e is the activity coefficient at the adsorption equilibrium, γ^0 is the activity coefficient at the standard state, and C^0 is the molar concentration of the standard reference solution (1 mol/L).

Substituting Eqs. (2.18) and (2.59) in Eq. (2.58), for very dilute solutions ($\gamma_e = \gamma^0$), Eq. (2.60) is obtained (Zhou et al. 2012):

$$K_e = \frac{\frac{q_e}{q_m}}{\left(1 - \frac{q_e}{q_m}\right)\frac{C_e}{C^0}} \tag{2.60}$$

or

$$q_e = \frac{q_m K_e \left(\frac{C_e}{C^0}\right)}{1 + K_e \left(\frac{C_e}{C^0}\right)} \tag{2.61}$$

In this way, the dimensionless K_e can be found by fitting of the Eq. (2.61) with the experimental data of q_e (mol/g) versus C_e (mol/L), considering $C^0 = 1$ mol/L. The regression and the parameter estimation should have good statistical indicators, as presented in Sect. 2.5.

After the correct estimation of the thermodynamic parameters, some important information about the adsorption can be obtained. For example, the negative values of ΔG^0 show a spontaneous and favorable process. The higher the ΔG^0 magnitude, the more favorable and spontaneous the adsorption. Negative values of ΔH^0 indicate an exothermic process, while positive values of ΔH^0 show an endothermic process. The magnitude of ΔH^0 can give an idea about the interactions that occur between the adsorbent and adsorbate. Physisorption, such as van der Waals interactions, is usually lower than 20 kJ/mol, and electrostatic interaction ranges from 20 to 80 kJ/mol. Chemisorption bond strengths can be from 80 to 450 kJ/mol. In relation to the ΔS^0, negative values show that the randomness decreases at the solid solution interface during the adsorption, and positive values suggest the possibility of some structural changes or readjustments in the adsorbate–adsorbent complex. Finally, if ΔH^0 contributes more than the $T\Delta S^0$ to find negative values of ΔG^0, the adsorption is an enthalpy controlled process; otherwise, if $T\Delta S^0$ contributes more than ΔH^0, the adsorption is an entropy controlled process (Crini and Badot 2008; Bergmann and Machado 2015).

2.7 Concluding Remarks

This chapter presented some fundamental aspects about the equilibrium isotherms in liquid phase adsorption, taking into account the academic and industrial viewpoints. In order to obtain accurate and correct interpretations about the adsorption

operation from the equilibrium isotherms, some paramount aspects should be remarked:

- The correct determination of the adsorption equilibrium requires at least 8 h of experiment. The experiments should be performed until the liquid phase concentration remains constant (coefficients of variation lower than 5%) after three consecutive measurements.
- The choice of the equilibrium models to be fitted with the experimental data cannot be performed indiscriminately. The experimental equilibrium curves should be classified according to the shape, and then only the adequate models should be used to fit the experimental data.
- For a correct parameter estimation from the isotherm models, the use of nonlinear estimation method is strongly suggested. To ensure the fit quality, the coefficient of determination (R^2) and at least one error analysis should be used. In some cases, the adjusted determination coefficient (R_{adj}^2) and AIC are also necessary.
- The Van't Hoff plot (ln (K_e) versus (1/T)) is a simple and reasonable way to find ΔH^0 and ΔS^0 values. However the equilibrium thermodynamic constant (K_e) should be used without units. Otherwise, the thermodynamic parameters have no sense.

References

Al-Ghouti MA, Allen SJ, Ahmad MN (2003) The removal of dyes from textile wastewater: a study of the physical characteristics and adsorption mechanisms of diatomaceous earth. J Environ Manag 69:229–238

Al-Qodah Z, Shawaqfeh AT, Lafi WK (2007) Two-resistance mass transfer model for the adsorption of the pesticide deltamethrin using acid treated oil shale ash. Adsorption 13:73–82

Anandkumar J, Mandal B (2011) Adsorption of chromium (VI) and rhodamine B by surface modified tannery waste: kinetic, mechanistic and thermodynamic studies. J Hazard Mat 186:1088–1096

Anderson DR, Burnham KP (2002) Avoiding pitfalls when using information-theoretic methods. J Wildl Manag 66:912–918

ASTM D3860-98 (2008) Standard practice for determination of adsorptive capacity of activated carbon by aqueous phase isotherm technique. ASTM International, West Conshohocken, PA, USA

ASTM D4607-94 (2006) Standard test method for determination of iodine number of activated carbon. ASTM International, West Conshohocken, PA, USA

Atkins P, De Paula J (2006) Atkins' physical chemistry. Oxford University Press, New York

Baccar R, Blánque P, Bouzid J, Feki M, Sarrá M (2010) Equilibrium, thermodynamic and kinetic studies on adsorption of commercial dye by activated carbon derived from olive-waste cakes. Chem Eng J 165:457–464

Bansal RC, Goyal M (2005) Activated carbon adsorption. CRC Press Taylor & Francis Group, New York

Bergmann CP, Machado FM (eds) (2015) Carbon nanomaterials as adsorbents for environmental and biological applications. Springer, Cham

Brunauer S, Emmett PH, Teller E (1938) Adsorption of gases in multimolecular layers. J Am Chem Soc 60:309–319

Cadaval TRS Jr, Dotto GL, Seus ER, Mirlean N, Pinto LAA (2016) Vanadium removal from aqueous solutions by adsorption onto chitosan films. Desalin Water Treat 57:16583–16591

Chen Y, Zhang D (2014) Adsorption kinetics, isotherm and thermodynamics studies of flavones from *Vaccinium bracteatum* Thunb leaves on NKA-2 resin. Chem Eng J 254:579–585

Crini G, Badot PM (2008) Application of chitosan, a natural aminopolysaccharide, for dye removal from aqueous solutions by adsorption processes using batch studies: a review of recent literature. Prog Polym Sci 33:399–447

Do DD (1998) Adsorption analysis: equilibria and kinetics. Imperial College Press, London

Dotto GL, Moura JM, Cadaval TRS Jr, Pinto LAA (2013) Application of chitosan films for the removal of food dyes from aqueous solutions by adsorption. Chem Eng J 214:8–16

Dotto GL, Nascimento dos Santos JM, Rosa R, Pinto LAA, Pavan FA, Lima EC (2015a) Fixed bed adsorption of methylene blue by ultrasonic surface modified chitin supported on sand. Chem Eng Res Des 100:302–310

Dotto GL, Sharma SK, Pinto LAA (2015b) Biosorption of organic dyes: research opportunities and challenges. In: Sharma SK (ed) Green chemistry for dyes removal from waste water: research trends and applications. Wiley, Hoboken, pp 295–329

Dotto GL, Sellaoui L, Lima EC, Ben Lamine A (2016a) Physicochemical and thermodynamic investigation of Ni(II) biosorption on various materials using the statistical physics modeling. J Mol Liq 220:129–135

Dotto GL, Meili L, de Souza Abud AK, Tanabe EH, Bertuol DA, Foletto EL (2016b) Comparison between Brazilian agro-wastes and activated carbon as adsorbents to remove Ni(II) from aqueous solutions. Water Sci Technol 73:2713–2721

Dotto GL, Rodrigues FK, Tanabe EH, Fröhlich R, Bertuol DA, Martins TR, Foletto EL (2016c) Development of chitosan/bentonite hybrid composite to remove hazardous anionic and cationic dyes from colored effluents. J Environ Chem Eng 4:3230–3239

Ebadi A, Soltan Mohammadzadeh JS, Khudiev A (2007) Adsorption of methyl tert-butyl ether on perfluorooctyl alumina adsorbents-high concentration range. Chem Eng Technol 30:1666–1673

Ebadi A, Mohammadzadeh JSS, Khudiev A (2009) What is the correct form of BET isotherm for modeling liquid phase adsorption? Adsorption 15:65–73

Edgehill RU (1998) Adsorption characteristics of carbonized bark for phenol and pentachlorophenol. J Chem Technol Biot 71:27–34

El-Khaiary MI, Malash GF (2011) Common data analysis errors in batch adsorption studies. Hydrometallurgy 105:314–320

Freundlich HMF (1906) Over the adsorption in solution. J Phys Chem 57:1100–1107

Geankoplis CJ (1998) Procesos de transporte y operaciones unitarias. Compañía Editorial Continental, Ciudad de México

Giles CH, MacEwan TH, Nakhwa SN, Smith D (1960) Studies in adsorption. Part XI. A system of classification of solution adsorption isotherms, and its use in diagnosis of adsorption mechanisms and in measurement of specific surface areas of solids. J Chem Soc 3973–3993

Hang TP, Brindley GW (1970) Methylene blue absorption by clay minerals. Determination of surface areas and cation exchange capacities. Clay Miner 18:203–212

Iram M, Guo C, Guan Y, Ishfaq A, Liu H (2010) Adsorption and magnetic removal of neutral red dye from aqueous solution using Fe_3O_4 hollow nanospheres. J Hazard Mat 181:1039–1050

Khraisheh MAM, Al-Ghouti MA, Allen SJ, Ahmad MN (2005) Effect of OH and silanol groups in the removal of dyes from aqueous solution using diatomite. Water Res 39:922–932

Kumar PS, Ramalingam S, Senthamarai C, Niranjanaa M, Vijayalakshmi P, Sivanesan S (2010) Adsorption of dye from aqueous solution by cashew nut shell: studies on equilibrium isotherm, kinetics and thermodynamics of interactions. Desalination 261:52–60

Langmuir I (1918) The adsorption of gases on plane surfaces of glass, mica and platinum. J Am Chem Soc 40:1361–1403

Li Q, Yue QY, Su Y, Gao BY, Sun HJ (2010) Equilibrium, thermodynamics and process design to minimize adsorbent amount for the adsorption of acid dyes onto cationic polymer-loaded bentonite. Chem Eng J 158:489–497

Lian L, Guo L, Guo C (2009) Adsorption of Congo red from aqueous solutions onto Ca-bentonite. J Hazard Mat 161:126–131

Liu Y (2009) Is the free energy change of adsorption correctly calculated? J Chem Eng Data 54:1981–1985

Marsal A, Bautista E, Ribosa I, Pons R, García MT (2009) Adsorption of polyphenols in wastewater by organo-bentonites. Appl Clay Sci 44:151–155

Milonjic SK (2007) A consideration of the correct calculation of thermodynamic parameters of adsorption. J Serb Chem Soc 72:1363–1367

Nabais JV, Mouquinho A, Galacho C, Carrott PJM, Ribeiro Carrott MML (2008) In vitro adsorption study of fluoxetine in activated carbons and activated carbon fibres. Fuel Process Technol 89:549–555

Nunes AA, Franca AS, Oliveira LS (2009) Activated carbons from waste biomass: an alternative use for biodiesel production solid residues. Bioresour Technol 100:1786–1792

Piccin JS, Vieira MLG, Gonçalves JO, Dotto GL, Pinto LAA (2009) Adsorption of FD&C red no. 40 by chitosan: isotherm analysis. J Food Eng 95:16–20

Piccin JS, Dotto GL, Vieira MLG, Pinto LAA (2011) Kinetics and mechanism of the food dye FD&C red 40 adsorption onto chitosan. J Chem Eng Data 56:3759–3765

Piccin JS, Feris LA, Cooper M, Gutterres M (2013) Dye adsorption by leather waste: mechanism diffusion, nature studies, and thermodynamic data. J Chem Eng Data 58:873–882

Redlich OJDL, Peterson DL (1959) A useful adsorption isotherm. J Phys Chem 63:1024–1024

Rodrigues AE (2015) Simulated moving bed technology: principles, design and process applications. Elsevier, Amsterdam

Rouquerol F, Rouquerol J, Sing KSW (eds) (2014) Adsorption by powders and porous solids: principles, methodology and applications. Elsevier, Amsterdam

Russo ME, Di Natale F, Prigione V, Tigini V, Marzocchella A, Varese GC (2010) Adsorption of acid dyes on fungal biomass: equilibrium and kinetics characterization. Chem Eng J 162:537–545

Ruthven DM (1984) Principles of adsorption and adsorption processes. Wiley, New York

Saad MEK, Khiari R, Elaloui E, Moussaoui Y (2014) Adsorption of anthracene using activated carbon and *Posidonia oceanica*. Arab J Chem 7:109–113

Sahadevan R, Mahendradas DK, Shanmugasundaram V, Shanmugam K, Velan M (2009) Sorption kinetics and equilibrium analysis for the removal of Reactive Red 2 and Reactive Blue 81 dyes from synthetic effluents using dried soya bean meal. Int J Chem React Eng 7:A33

Shafeeyan MS, Daud WMAW, Shamiri A (2014) A review of mathematical modeling of fixed-bed columns for carbon dioxide adsorption. Chem Eng Res Des 92:961–988

Smith JM, Van Ness HC, Abbott MM (2005) Introduction to chemical engineering thermodynamics. McGraw-Hill, Columbus

Suzuki M (1993) Fundamentals of adsorption. Elsevier, Amsterdam

Van den Hul HJ, Lyklema J (1968) Determination of specific surface areas of dispersed materials. Comparison of the negative adsorption method with some other methods. J Am Chem Soc 90:3010–3015

Vázquez G, González-Álvarez J, Garcia AI, Freire MS, Antorrena G (2007) Adsorption of phenol on formaldehyde-pretreated Pinus pinaster bark: equilibrium and kinetics. Bioresour Technol 98:1535–1540

Vieira MLG, Esquerdo VM, Nobre LR, Dotto GL, Pinto LAA (2014) Glass beads coated with chitosan for the food azo dyes adsorption in a fixed bed column. J Ind Eng Chem 20:3387–3393

Weber CT, Collazzo GC, Mazutti MA, Foletto EL, Dotto GL (2014) Removal of hazardous pharmaceutical dyes by adsorption onto papaya seeds. Water Sci Technol 70:102–107

Wong YC, Szeto YS, Cheung W, McKay G (2004) Adsorption of acid dyes on chitosan-equilibrium isotherm analyses. Process Biochem 39:695–704

Worch E (2008) Fixed-bed adsorption in drinking water treatment: a critical review on models and parameter estimation. J Water Supply Res T 57:171–183

Yousef RI, El-Eswed B, Ala'a H (2011) Adsorption characteristics of natural zeolites as solid adsorbents for phenol removal from aqueous solutions: kinetics, mechanism, and thermodynamics studies. Chem Eng J 171:1143–1149

Yuvaraja G, Krishnaiah N, Subbaiah MV, Krishnaiah A (2014) Biosorption of Pb (II) from aqueous solution by *Solanum melongena* leaf powder as a low-cost biosorbent prepared from agricultural waste. Colloid Surf B 114:75–81

Zhang Y, Yan L, Xu W, Guo X, Cui L, Gao L, Wei Q, Du B (2014) Adsorption of Pb (II) and Hg (II) from aqueous solution using magnetic $CoFe_2O_4$-reduced graphene oxide. J Mol Liq 191:177–182

Zhang Y, Wang W, Zhang J, Liu P, Wang A (2015) A comparative study about adsorption of natural palygorskite for methylene blue. Chem Eng J 262:390–398

Zhou X, Liu H, Hao J (2012) How to calculate the thermodynamic equilibrium constant using the Langmuir equation. Adsorpt Sci Technol 30:647–649